

# Thermal Modelling of Buildings

Daniel Ryder-Cook

Supervisor : Prof David MacKay

May 11 2009

## Abstract

The aim of this project was to make a series of thermal models to describe the form of temperature variation within buildings. This would then be used to gain information about the buildings physical properties and the methods of heat generation. To do this, empirical models with adjustable parameters were developed to account for the suspected leading order terms in heat loss and production within the building. The distribution of the most likely values for empirical parameters was found by employing Bayes' theorem with a long-tailed likelihood and sampling intelligently from the posterior probability distribution using slice sampling (a Markov-Chain Monte-Carlo technique). Heat losses were modelled in terms of convection and conduction by heat exchange with the environment and with other compartments. This approach showed a good correspondence with our prior physical estimates and the inferred rate of cooling. From the heat loss models, physical parameters of the building such as its transmittance became possible to estimate. Heat generation models considered a uniform heat source for which the power consumption was measurable and this again showed reasonable agreement with prior physical estimates. Finally the model was extended to take account of incident solar radiation, which was observed to have a small but measurable effect on the form of the temperature variation.

## 1. Introduction

When developing strategies to minimise energy consumption within buildings it is crucial to understand the dynamics of energy generation and loss. This project aims to investigate some of the contributions to heat generation and loss studied through the development of a number of empirical models. From these models of the heat flows within a building a thermal model may be derived allowing us to relate heat flows to the variations in temperature. The models developed will have adjustable parameters corresponding to different contributions to the heat budget and so by accurately understanding the form of temperature variation we aim to appreciate the most important factors in the energy consumption and production within the building.

Using these thermal models in combination with natural data (e.g. raw temperature data from the building and data from weather stations) the objectives of the project are:

1. To infer thermal properties of the buildings – primarily achieved by modelling the process of heat loss within a building.
2. To infer heat production (i.e. to make a virtual energy meter) – primarily achieved by looking at possible models of contributions to heat production.

What might we expect this thermal model to look like? Well, we need to think about the most obvious causes of heat generation and loss within a building. Firstly looking at heat losses, these can be generally categorised into two forms, conduction and ventilation. Conductive heat losses can be thought of in terms of heat flowing from a hot region to a cold region through windows and walls. Ventilation meanwhile represents the direct movement of hot air out of a building through cracks and gaps as well as through deliberate ventilation. The standard method of modelling such heat losses is to make both heat flows proportional to the temperature difference between the two regions. In this investigation we will primarily be concerned with modelling those losses that are the result of conduction as in a typical British house, it is these which will be dominant [1]. In addition to heat losses we will also need to consider how heat is generated within buildings to replenish that which is lost. Particular sources of interest will include the buildings' heating system and the effect of sunlight as well as the effect of the buildings' occupants and the many heat generating devices which are common inside most British homes

A mathematical formulation of the problem will take a general form where the rate of change in the heat is related to functions of the temperature and time that are likely to describe heat losses, as well as functions which are not directly related to the temperature but which describe many of the terms responsible for heat generation.

$$\frac{dQ}{dt} = A(T, t) + B(t)$$

Where the function  $A(T, t)$  (dependent on temperature and time) encompasses all information regarding heat loss and  $B(t)$  (dependent on time only) encompasses all information regarding heat generation.

However, it is more convenient to measure the temperature within a compartment of a building. We therefore make the assumption that  $\Delta Q(t) = C\Delta T(t)$  where  $C$  is a measure of the heat capacity of the compartment otherwise known as its thermal mass. In effect a compartment may be treated as a reservoir of heat with uniform temperature.

$$\frac{dT}{dt} = \frac{1}{C} (A(T, t) + B(t))$$

The exact form of this differential equation will depend on the contributions that are included but in general we will be looking to find the best fit of a many parameter model that includes terms relating both to heat generation and losses. From these models, using numerical integration (see appendix A), we will be able to generate theoretical values of the temperature variation and so perform statistical comparison with the collected data.

Faced with the task of assigning preferences to alternative models of varying complexity, the process of data modelling is approached using a Bayesian methodology for inference for the different multivariable models of temperature variation.

## 2. Bayesian methodology for inference

### 2.1 Bayes Theorem and Parameter Estimation

The process of data modelling can often be distinguished into two different processes. The first stage is fitting the model to the data. In this stage we assume a particular model to be true and infer what values its free parameters may plausibly take, given the data. The second stage is that of model comparison where different models are compared and ranked according to their fit of the data. Within this project we will be primarily concerned with the first of these tasks. It should be noted that the aim of our inference is not only the most probable fit of the data (although this will be of interest) but to assess the whole distribution of probabilities for multiple values of the parameters.

To fit a model to the data we employ Bayes theorem. This states that the posterior probability of the parameters  $\theta$  given the data  $D$  is given by:

$$P(\theta|D, H_i) = \frac{P(D|\theta, H_i)P(\theta|H_i)}{P(D|H_i)} \quad [2]$$

that is,

$$\text{Posterior} = \frac{\text{Likelihood} \times \text{Prior}}{\text{Evidence}}$$

The Prior represents what we know about the parameters before we look at the data. The likelihood represents what we learn about the parameters when we take the data into account and the evidence is a normalising constant. In most situations unless otherwise stated we will assume a uniform prior and so a pretty much direct relationship between the likelihood and the posterior other than a normalising constant.

### 2.2 Calculating Likelihoods

The likelihood function (which encodes the information we obtain about the parameters from looking at the data) for a dataset  $\{x_n\}$  and a set of parameters  $\theta$  will in general be given by:

$$P(\{x_n\}|\theta) = \prod_i P(x_i|\theta) \quad [3]$$

But what do we take as the value of  $P(x_i|\theta)$ ? To fit the model to the data we need to use a suitable probabilistic model of how the data will differ from the calculated values. It should be noted that because we are working with a product sum and for any reasonable amount of data it is much safer to work with the log of the likelihood as this allows us to express our product as a straightforward sum with which we are less likely to encounter problems in the computational implementation of the procedure.

$$-\log P(\{x_n\} / \theta) = -\sum_i \log P(x_i / \theta)$$

One very widely used distribution to describe deviations is the Gaussian distribution. It is true that in many situations, where the errors are random and there are a large number of measurements, this may be appropriate. The mathematical form of this distribution will be:

$$P(T_i / \theta) = \frac{1}{\sqrt{2\pi}\sigma} \exp\left(-\frac{(T_{Theory}(\theta) - T_i)^2}{2\sigma^2}\right)$$

Where  $T_i$  are the collected temperature data and  $T_{Theory}(\theta)$  are theoretical values calculated by numerical integration of the differential equation governing temperature variation (see Appendix A for details of the technique for numerical integration). For details of the sources used to collect relevant data, see Appendix B.

However, one major problem with this distribution is the effect that outliers may have. The light tails of the Gaussian distribution, where deviations from the expected value become incredibly rare, can cause an outlier to dramatically reduce the probability of a particular set of parameters. To visualise this problem we may think of  $\varphi(\Delta x) = -\log(Likelihood)$  as a physical potential and  $\nabla\varphi$  as a force with which each datum pulls on the model. This results in a quadratic variation in the log of the likelihood or rather a linear increase in the force exerted by datum as they fall further from the mean [4].

To overcome this problem we need to consider possible distributions which are more tolerant of outliers and so we look to distributions with heavier tails. One such example distribution would be a mixture of Gaussians. In particular we use the simple Long-tail Likelihood of a mixture of two Gaussians. The mathematical form for this distribution will be:

$$P(T_i / \theta) = \frac{1-\beta}{\sqrt{2\pi}\sigma} \exp\left(-\frac{(T_{Theory}(\theta) - T_i)^2}{2\sigma^2}\right) + \frac{\beta}{\sqrt{2\pi}\sigma\gamma} \exp\left(-\frac{(T_{Theory}(\theta) - T_i)^2}{2\sigma^2\gamma^2}\right) \quad [5]$$

Where typical values parameters are  $\sigma = 3$ ,  $\beta = 0.01$  and  $\gamma = 5$  which embodies our anticipation that simple models may reasonably have errors of the order  $\pm 3^\circ K$  while also ensuring outliers do not lead distortion of the distribution up to  $\pm 15^\circ K$

### 2.3 Slice Sampling

Although we can calculate the probability density function at any particular point of the parameters it becomes increasingly difficult to enumerate all hypotheses as the number of parameters increases. We can save a lot of time by honing in on hypotheses that fit the data well. Slice sampling is a Markov-Chain Monte-Carlo technique that adapts to the distribution being sampled using the principle that one can sample efficiently from a distribution by sampling uniformly from the region under the plot of the density function [6].

How does it work? Well, a Markov-Chain that converges to this uniform distribution can be constructed by alternating uniform sampling in the vertical direction with uniform sampling from the current vertical slice.

To appreciate this, let's go through the procedure for a univariate (1-dimensional distribution). Within one dimensional slice sampling transitions are made from a two dimensional point  $(x,y)$  lying under the curve  $P^*(x)$  to another point  $(x',y')$  lying under the same curve such that the distribution of points  $(x,y)$  tends to a uniform distribution over the area under the curve.

The procedure is as follows:

- a) Starting at  $x_0$ , a vertical level  $y$  is drawn uniformly from  $(0, P^*(x_0))$  and used to define a horizontal slice

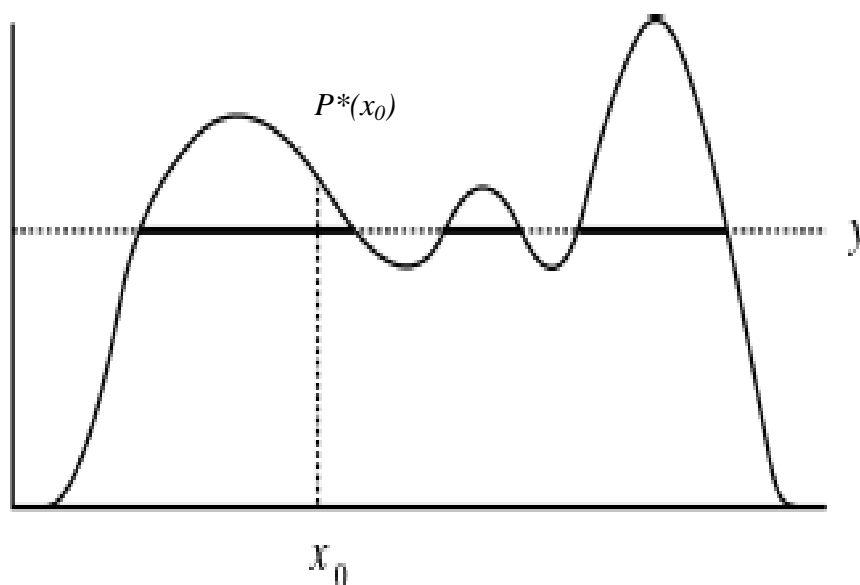


Figure 2.31 – shows a schematic for the initial drawing of the slice

An interval of width  $w$  is randomly placed about  $x_0$  and then expanded in steps until both sides are outside the slice. One of the more efficient methods of ensuring we enclose a large amount of the slice is the doubling procedure of stepping out. That is the interval is doubled until both ends are outside the slice.

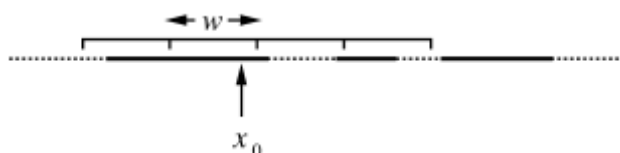


Figure 2.32 [adapted from 6]

A new point  $x_1$  is found by picking uniformly from the interval until a point inside the slice is found. Points picked that are outside the slice (where the lines are dotted) are used to shrink the interval.

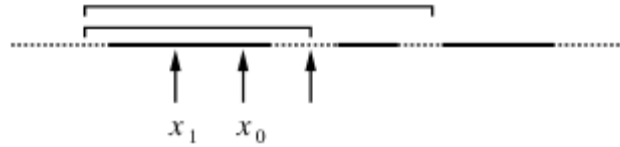


Figure 2.33 [adapted from 6]

For the interval  $I$  the set of acceptable successor states is defined by

$$A = \{x : x \in S \cap I \text{ and } P(\text{select } I / \text{at state } x) = P(\text{select } I / \text{at state } x_0)\}$$

The above algorithm is implemented in python and the results of the sampling are plotted in Gnuplot. See Appendix D for further details.

### 3. Thermal models

A number of different thermal models will now be presented and applied in different situations to gain information about the thermal properties of buildings and to characterise heat generation. In each case the theoretical basis for the model is presented along with a test of the program with toy data. We then look at the application of the program to real data and the consequent estimation of the contributions to the heat budget.

#### 3.1 One parameter cooling

To try and infer the thermal properties of buildings we first look at periods of time where we are sure that all sources generating heat within the building are reduced to zero. This then allows us to focus solely trying to understand the mechanism for heat loss. An example of when this might occur would be a period where the occupants of the building are away and all heat generating devices are switched off. In this situation we can build a simple model which assumes that initially, the inside of the compartment is at a higher temperature than the outside of the compartment and, that the heat loss will be related to this temperature difference (Figure 3.11 shows a toy model of this situation).

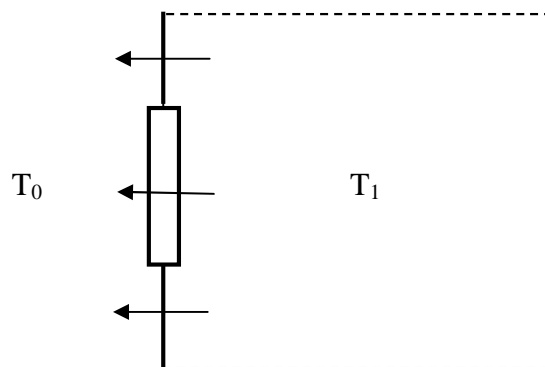


**Figure 3.11 Shows toy model of the situation with a compartment only exchanging heat with the outside environment and not with adjacent compartments within the building. Heat flows are represented with arrows and in this figure two surfaces for heat loss are provided, that of a wall and that of a window.**

The resulting heat flow from hot region to cold region which may be described by:

$$\frac{dQ}{dt} = -\sum_i h_i A_i (T(t) - T_0(t)) \quad [1]$$

where  $T(t)$  is the temperature inside the compartment, and  $T_0(t)$  is the temperature of the outside environment.  $A_i$  represents the surface area of one of the surfaces within the model over which heat is being lost and  $h_i$  represents a measure of the thermal transmittance for that surface with units of  $\text{Wm}^{-2}\text{K}^{-1}$ . High values of the transmittance correspond to bigger losses of heat and typical values range from  $0.6 \text{ Wm}^{-2}\text{K}^{-1}$  for an insulated cavity block-brick wall to  $5 \text{ Wm}^{-2}\text{K}^{-1}$  for a single glazed window [7]. We may further assume that the body has a sufficiently good thermal conductivity that to a good approximation we can consider the body to be at a uniform temperature. In such cases the entire body is treated as a lumped capacitance reservoir of heat i.e.  $\Delta Q = C\Delta T$  where  $C$  is the heat capacity with units  $\text{JK}^{-1}$ . As a result we obtain Newton's law of cooling to describe the differential form of temperature variation with time:

$$\frac{dT}{dt} = -\alpha (T(t) - T_0(t))$$

Where

$$\alpha = \frac{\sum_i h_i A_i}{C}$$

Where, the parameter  $\alpha$  characterises the rate of cooling and has units of  $\text{s}^{-1}$ . Before proceeding with the inference of the parameters let us first use our physical understanding of the situation to get an estimate for the value of  $\alpha$ . To obtain an estimate we simply substitute reasonable values into the above expression. First considering the numerator we see in the toy model there are two surfaces for exchange, a window of typical size  $2\text{m}^2$ , and a wall of size  $10 \text{ m}^2$ . Appropriate values for the thermal transmittance are  $5 \text{ Wm}^{-2}\text{K}^{-1}$  and  $1 \text{ Wm}^{-2}\text{K}^{-1}$  respectively. This yields a numerator with a value of  $20 \text{ WK}^{-1}$ . To calculate the heat capacity of the room we will need to consider a number of factors including, the heat capacity of the air in the room, the heat capacity of the stuff in the room (e.g. furniture, personal possessions etc...) and the effect of ventilation has on the heat capacity. The details of this calculation are contained in appendix C and yield a value of  $C_{Total} = 1 \times 10^7 \text{ JK}^{-1}$ . with this we may estimate a value of  $\alpha$  to be  $2 \times 10^{-6} \text{ s}^{-1}$  or  $0.008 \text{ hour}^{-1}$ . Note, this is highly dependent on the estimate of the room's heat capacity.

As a way of testing the program is functioning correctly a number of simulations were carried out on toy data to ensure that parameter prediction was achieved correctly before applying the simulation to real data. Figure 3.12 shows an example of one such test where toy data has been generated from known values of the parameters.

Figure 3.13 shows a comparison of the toy temperature data with the theoretically predicted values at the maximum of the likelihood. The increase in temperature at the end of this plot is related to the increase of the outside temperature in the toy data in the latter half of the time series.

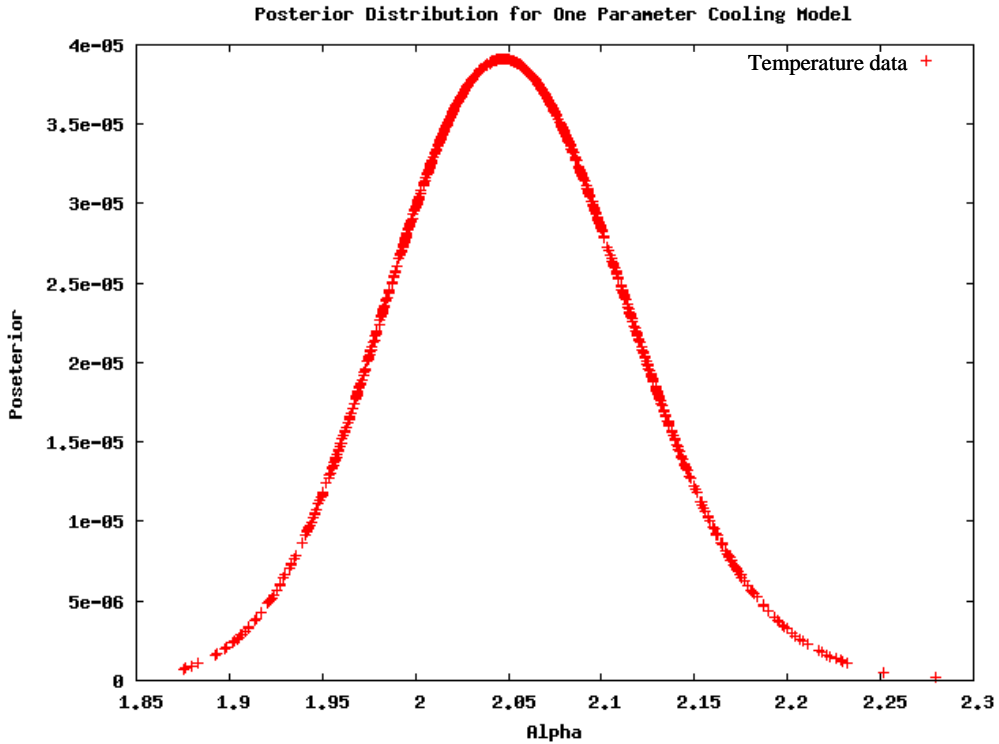


Figure 3.12 – Plot of the Posterior distribution for the case of  $\alpha = 2.05$ . It should be noted that for this simple one dimensional distribution for a small number of data points we are able to plot the posterior directly. However for larger numbers of data points and parameters we will need to work with the log of the likelihood in the plotting as we have done throughout in the implementation of slice sampling.

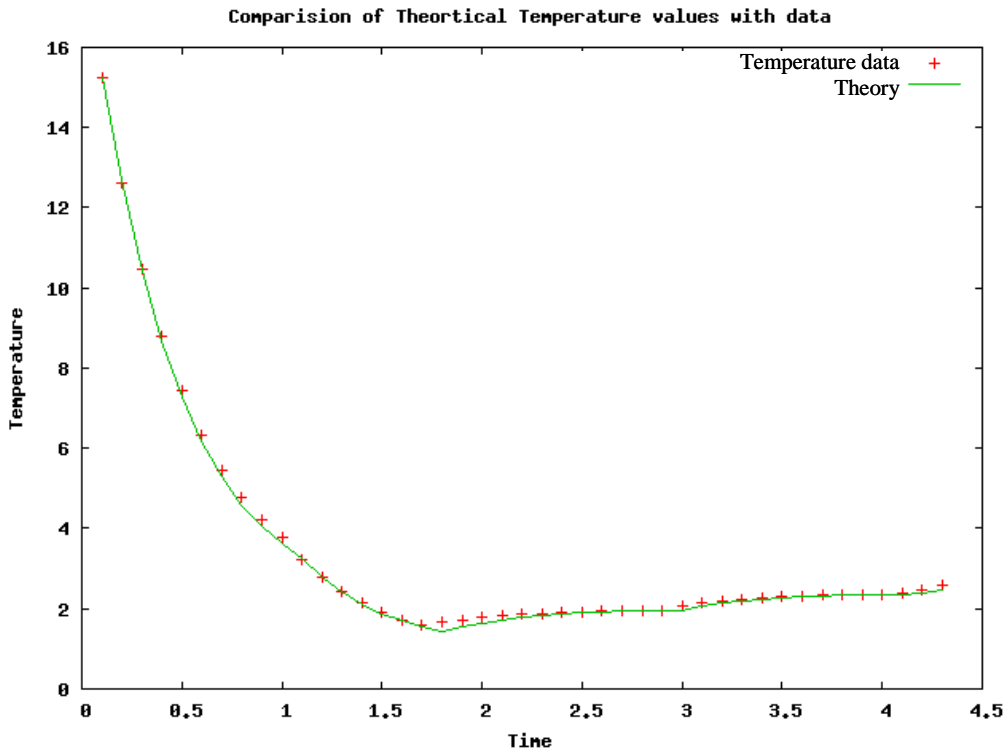


Figure 3.13 – Comparison between theoretical values and the data for the test of the inference algorithm with a known value of the parameter.

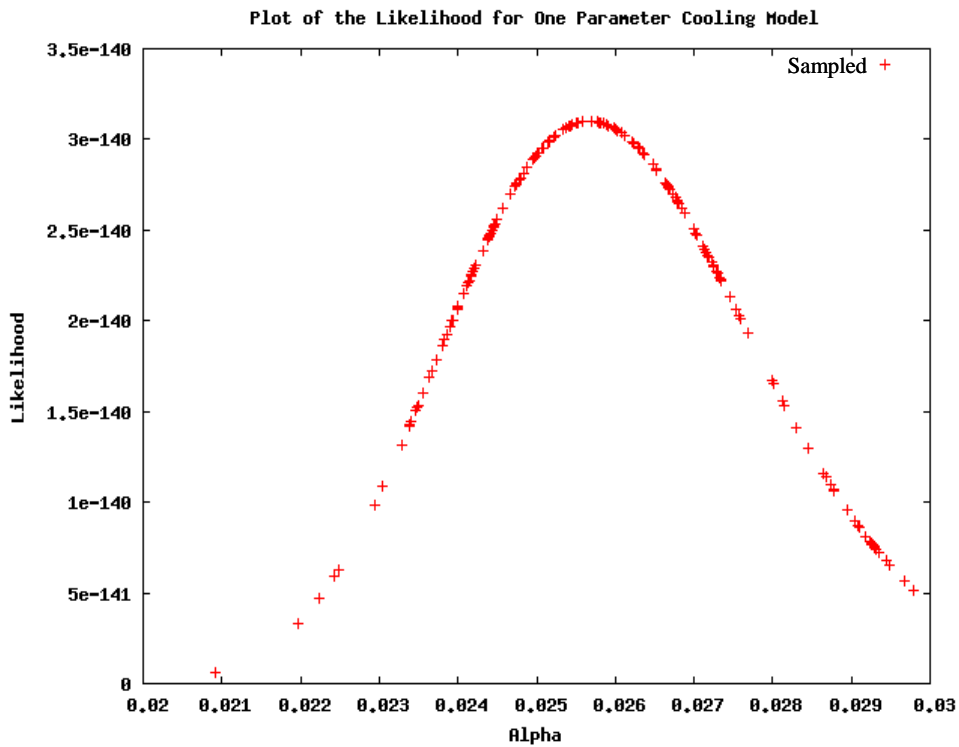


Figure 3.14 – plot of sampled values from the log of the posterior distribution for the parameter  $\alpha$  for the period of cooling.

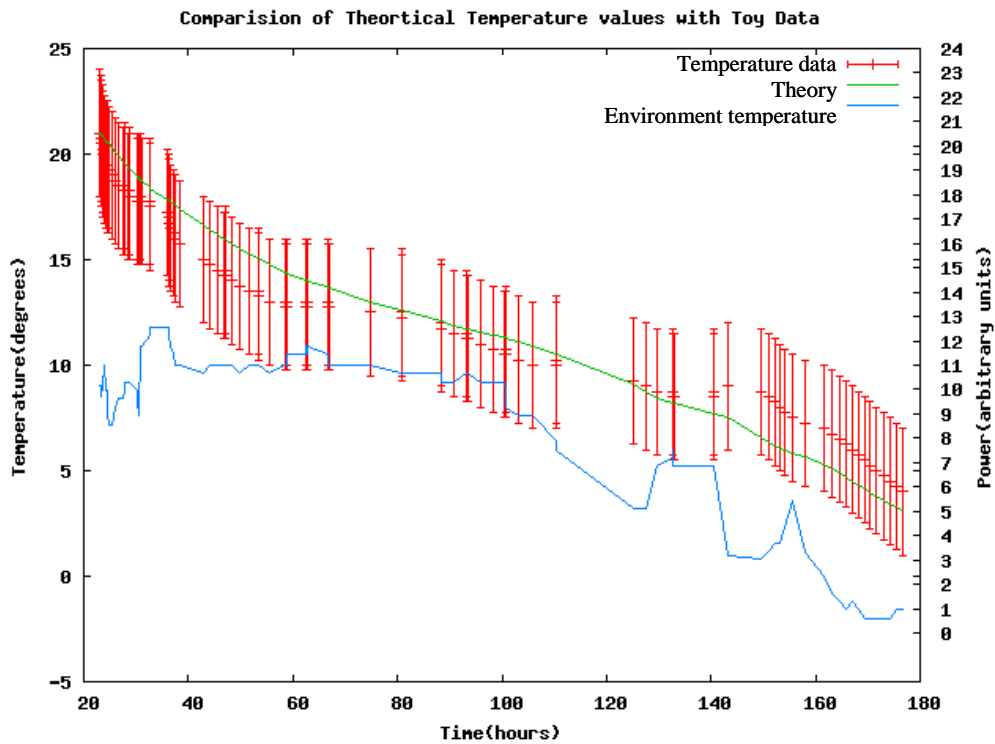


Figure 3.15 – plot showing the variation of the temperature over the cooling period and the corresponding theoretical fit of the data. Note also shown is the variation in outside temperature

Turning our attentions to the real data, temperature variation was investigated over a period when the building was empty and all heat generation sources were known to have been switched off or removed. As a result the building was allowed to cool freely through interaction with the environment. Figure 3.15 shows a plot of the posterior distribution. For the set of data provided the maximum likelihood was found to be at  $\alpha = 0.026 \text{ hour}^{-1}$  in reasonable correspondence with the predicted value of  $0.008 \text{ hour}^{-1}$ .

It seems clear that the above model although on the right track it is failing to predict the small scale variations in the temperature as compartment cools. This failing is likely due to incorporating wide range of causes of heat loss into a single parameter when in fact a room such as the one considered will have many smaller contributions to heat loss than just Transfer across one surface. This fact is additionally seen with the inferred parameter  $\alpha = 0.026 \text{ hour}^{-1}$  being  $\sim$  a factor of 3 higher than the typical value predicted in the earlier estimation  $0.008 \text{ hour}^{-1}$ . A potential alternative is to increase the complexity of the mechanism by which our compartment interacts with the environment. To do this we will need to consider the idea of adjacent compartments with which there will likely be conduction with in a normal building.

### 3.2 Two Compartment Cooling

A simple example of a more complex model of cooling consider a two compartment situation where the room is divided into two compartments one being the inside of the room and the other being some additional structure like a wall. A schematic of a toy physics model of this situation is shown in figure 3.21.

The above model now allows not only for direct losses to the environment but also and interaction with a compartment with a markedly different heat capacity. This will modify the cooling curve in general into a superposition of an initially dominant fast cooling which is later overtaken by a slower rate of cooling response

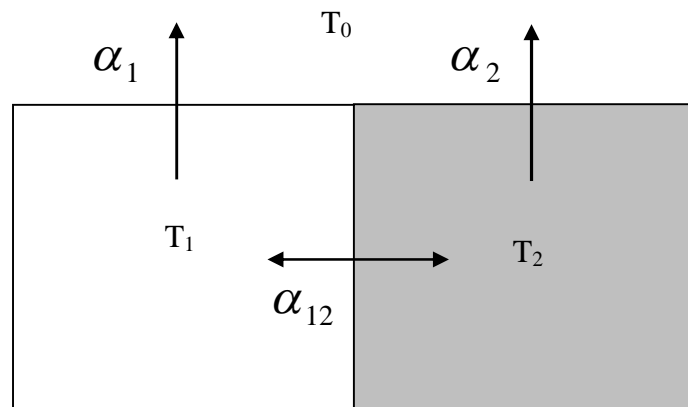


**Figure 3.21 showing a more complex approach to modelling cooling where compartment 1 represents the room and compartment 2 represents a structure like a wall.**

We subsequently obtain two differential equations for the compartments:

$$\frac{dT_1}{dt} = -\alpha_1(T_1(t) - T_0(t)) - \alpha_{12}(T_1(t) - T_2(t)) \quad \text{where } T_1 = \frac{Q_1}{C_1}$$

$$\frac{dT_2}{dt} = -\alpha_2(T_2(t) - T_0(t)) + \alpha_{12}(T_1(t) - T_2(t)) \quad \text{where } T_2 = \frac{Q_2}{C_2}$$

It is worth noting that the large heat capacity of the wall like structure will be much larger any so an influx of heat from the room will have a much smaller effect on the temperature of the wall. For this reason although we do not have data for the temperature of the wall we can assume that it is somewhere between that of the room and the environment and that it is roughly constant to a first approximation. Values for  $\alpha_1$  and  $\alpha_{12}$  can be calculated as they were previously and we would expect values comparable to that calculated in section 3.1 i.e.  $\alpha \sim 0.01 \text{ hour}^{-1}$ .

Again the simulation is first tested using toy data generated from known parameters. As we have moved to a 3 dimensional hypothesis space forming a plot of the likelihood is not feasible as it was before and so only a comparison of the data with the theoretical prediction is provided (see Figure 3.22). From this we can see that slice sampling still makes accurate predictions as we are moving into higher dimensional hypothesis space.

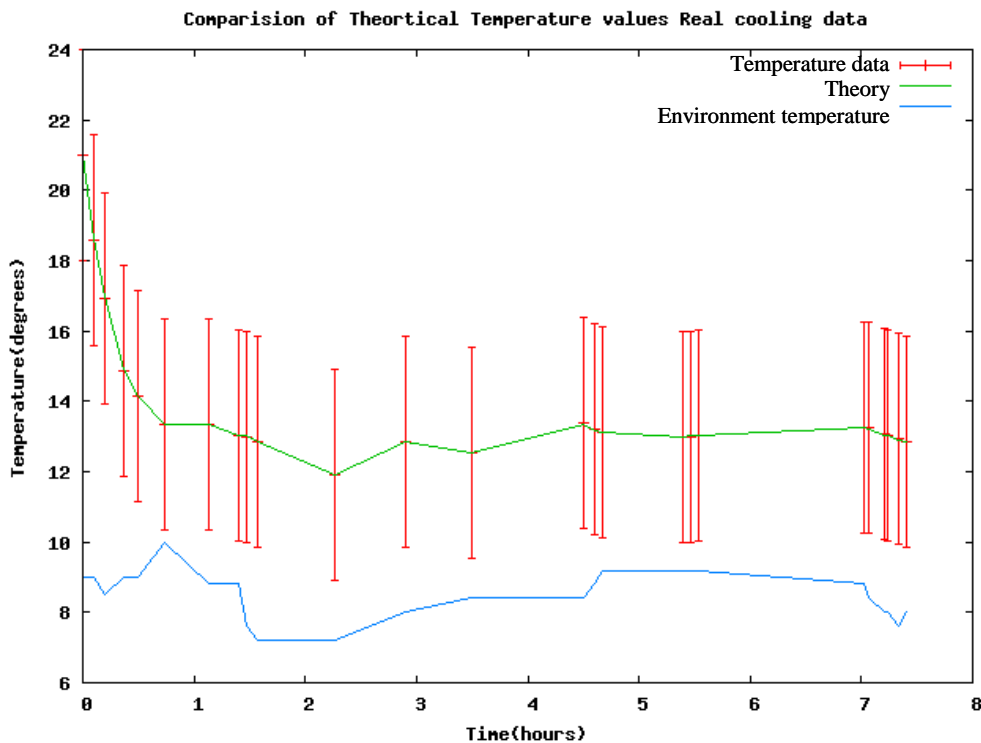


**Figure 3.22 - Plot of the comparison between theoretical values and the toy data generated from the Parameters  $\alpha_1 = 1 \text{ s}^{-1}$   $\alpha_2 = 0.1 \text{ s}^{-1}$   $\alpha_{12} = 2 \text{ s}^{-1}$  provided as a means of testing the correct functioning of the program.**

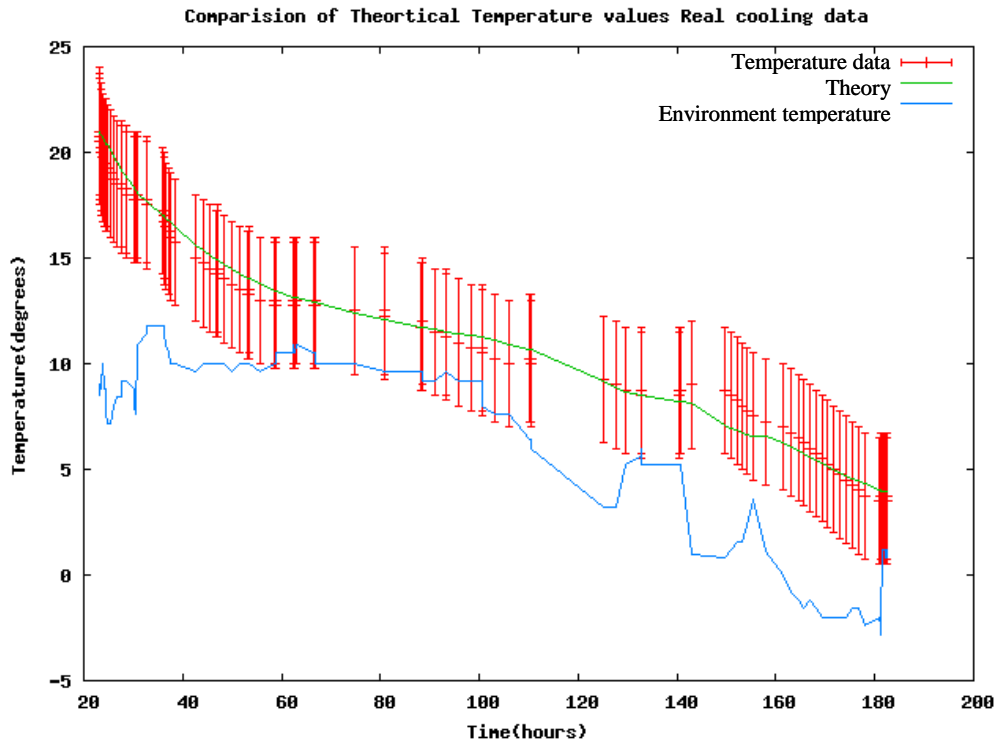


**Figure 3.23 - Plot of the comparison between theoretical values and the data for the test of the program with Real Data.**

With the application of this new model to the data, the parameters reach a maximum likelihood at  $\alpha_1 = 0.027 \text{ hour}^{-1}$  and  $\alpha_{12} = 0.013 \text{ hour}^{-1}$ . The value of  $\alpha_2$  has no effect on the temperature variation within this model as the temperature  $T_2$  is taken to be constant

As we can see there is an improvement in the fit of the theoretical curve however the inferred values of the parameters are still higher than those expected implying that our mechanism for cooling is still trying to incorporate many different effects into a small number of parameters forcing these parameters to be larger.

A possible solution to this is to build a full scale interacting compartment model where each room within the building can interact with all of the other rooms and also with the environment. Such a model would give a more accurate representation of the dynamics of heat loss and would be an interesting point of further investigation. A possible mathematical form for such a model might be:

$$\frac{dT_i}{dt} = u_i(t) + k_{i1}(T_i - T_1) + k_{i2}(T_i - T_2) \dots k_{in}(T_i - T_n)$$

Where  $u_i(t)$  represents contributions to temperature variation specific to compartment  $i$  which are not directly related to other compartments. In addition a more complex model of the wall like structure beyond something with a uniform block at a fixed temperature would also be an interesting point of further investigation.

### 3.3 One parameter cooling and power generation

As stated previously a key contribution to the model of temperature variation involves the inclusion of various heat sources from within the compartment. One such source, likely to be important is that of the buildings heating system. The simplest model relating the power input of the heating system to that of the generation of heat within a compartment will be that of a time dependent source generating heat uniformly across the compartment. It should be noted that this model neglects factors like air movement or position of the source. The primary aim of this model is to act as a first order approximation of the effect of a source delivering power on the temperature. Generation of heat by the source may be described according to:

$$\frac{dQ_{\text{Heating}}}{dt} = \eta P(t)$$

Where  $\eta$  is a coefficient of the efficiency define by:

$$\eta = \frac{\text{Power Delivered}}{\text{Power Consumed}}$$

And  $P(t)$  represents the power consumed. As a result the variation in the temperature can be described by the differential form:

$$\frac{dT}{dt} = -\alpha (T(t) - T_0(t)) + \beta P(t)$$

Where the coefficient  $\beta$  is a measure of the efficiency with which the heating system can raise the temperature of the compartment given the power consumed and is defined as  $\beta = \frac{\eta}{C}$  where  $C$  is again the heat capacity of the room. In the above

expression the terms associated with cooling have their previous meaning. A simple real life example of this kind of source might be the use of a gas fire. In this case the efficiency coefficient will simply be the efficiency of the gas fire in converting the calorific content of gas into heat within the room. For a gas fire which can either be on, burning gas at a constant rate, or off, burning no gas the Power function  $P(t)$  will be a periodic step function. An illustration of the behaviour of this function is represented in figure 3.31.

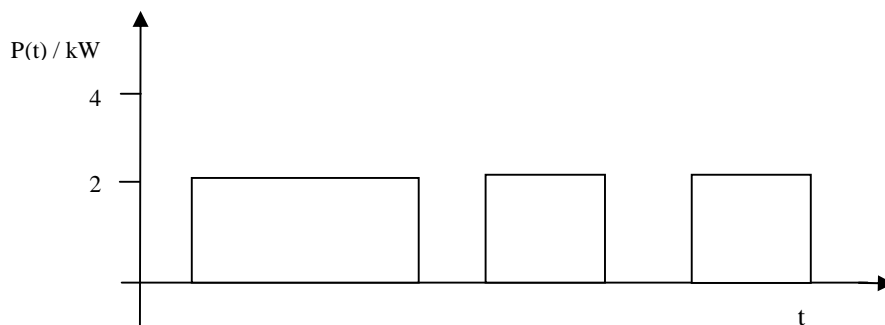


**Figure 3.31 – Illustration of the expected functional form of the Power**

Again before we go forward with the inference of the parameters for this situation it will be useful to make a ballpark estimate of what value we might expect the parameter  $\beta$  to take. For the case of the gas fire we would expect approximately a 2kW power supply when on and perhaps an efficiency of at best 0.8. We are then able to make use of the heat capacity we found for the room in section 3.1 (see appendix C). With this, we find an estimate of  $\beta = 8.89 \times 10^{-8} \text{ KJ}^{-1}$  or for time variations measured in hours  $\beta = 3.2 \times 10^{-4} \text{ KJ}^{-1}$ .

Again we test the correct functioning of the program with some toy data for which we know the input parameters which have generated the data. To represent the posterior distribution in the now two dimensional hypothesis space two different types of plots may be used. Figure 3.31 shows a surface plot of the data points for a number of different orientations of the x-y-z axes and Figure 3.32 shows the same situation represented as a contour plot.

As with the cooling model looking at a comparison of predicted temperature variation for parameters with maximum likelihood and the toy data generated provides a useful check that the algorithm is honing in on the appropriate hypotheses (see Figure 3.33).

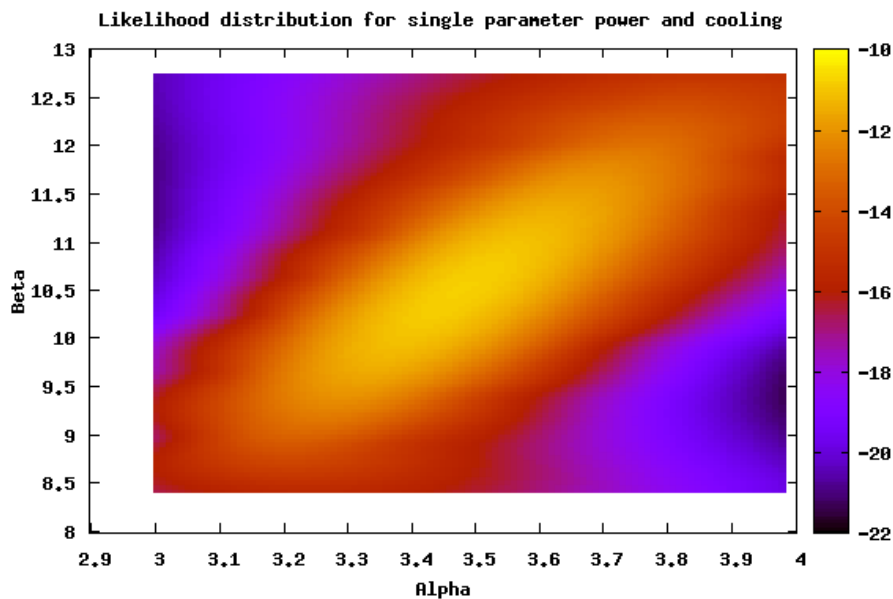


**Figure 3.32 – shows a contour plot of the log of the likelihood distribution found by the sampling algorithm, for parameters  $\alpha = 3.5 \text{ s}^{-1}$   $\beta = 10.5 \text{ KJ}^{-1}$**

To investigate real data a period in November was chosen to record all uses of the gas fire, along with the duration and the volume of gas used. With this data we were then able to apply the above model to the temperature data. Figures 3.34A-B shows surface plots of the log of the likelihood for a number of different orientations. The likelihood was found to be maximised for parameter values  $\alpha = 0.013 \text{ hour}^{-1}$ ,  $\beta = 1.9 \times 10^{-4} \text{ KJ}^{-1}$  (corresponding to an efficiency of 47% for the gas fire).

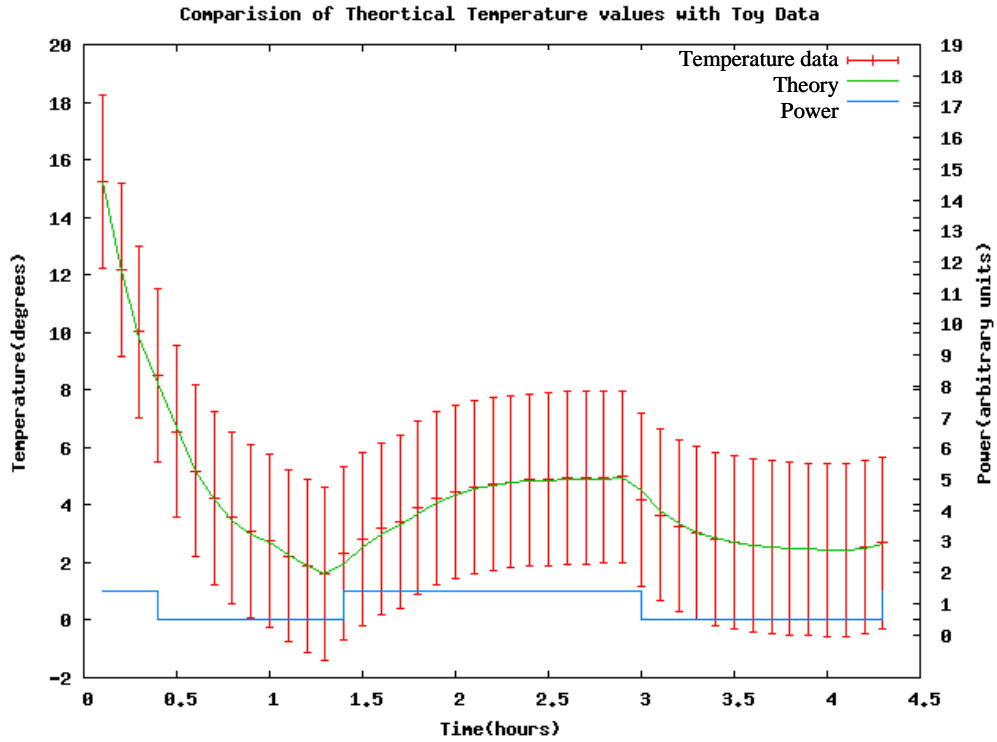


Figure 3.33 – – Plot showing the values of the data and the corresponding theoretically predicted values. In addition, the power function is also plotted for comparison.

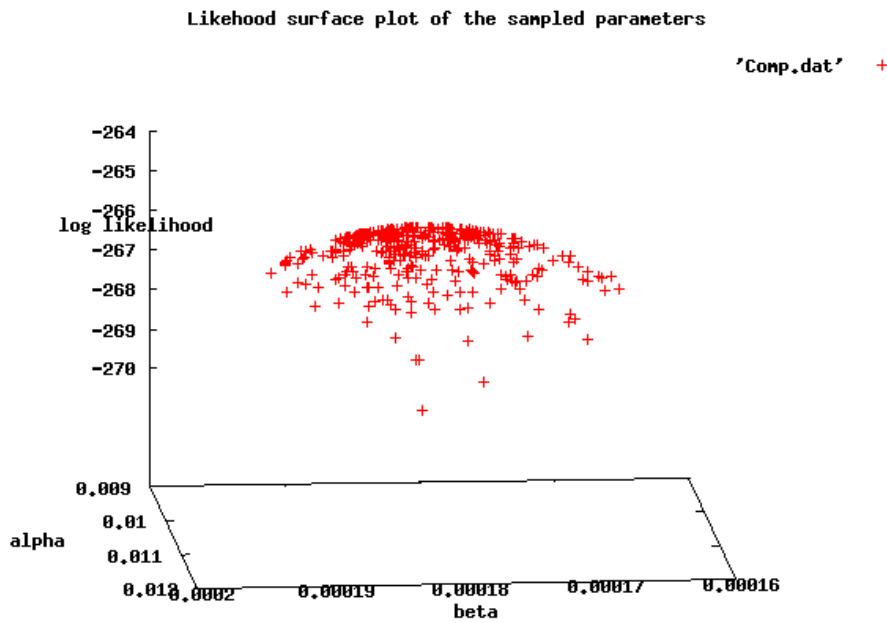
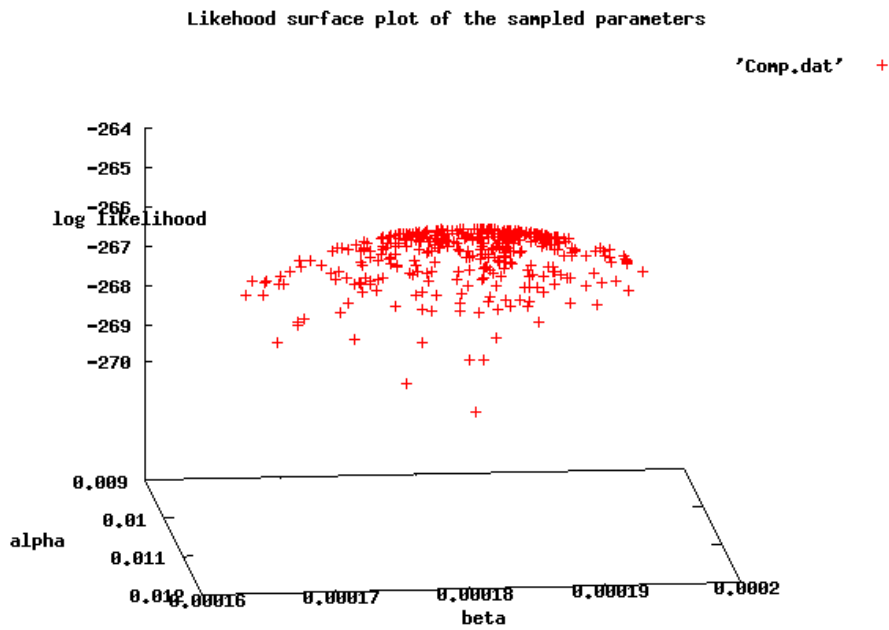
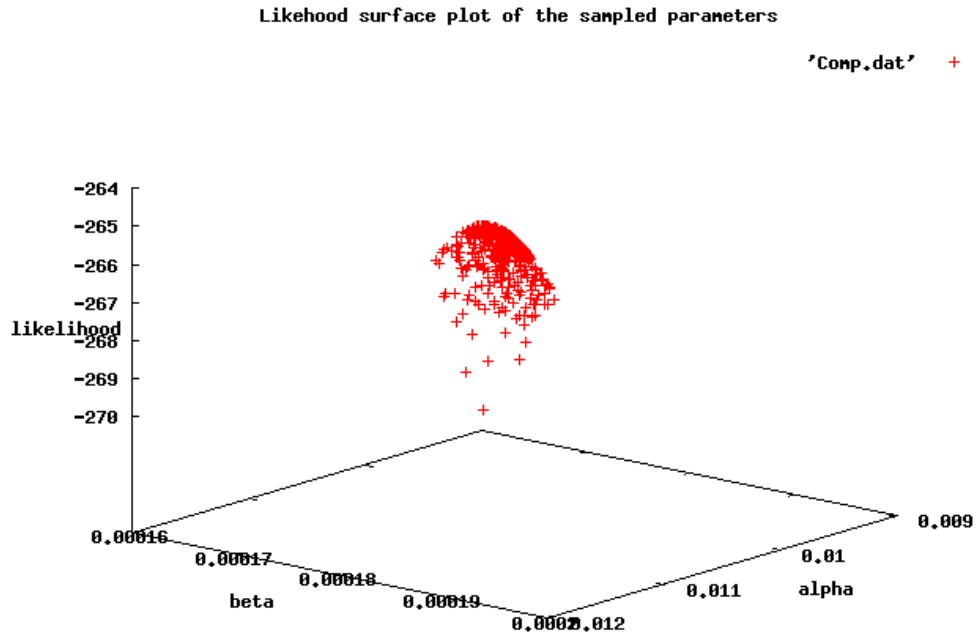
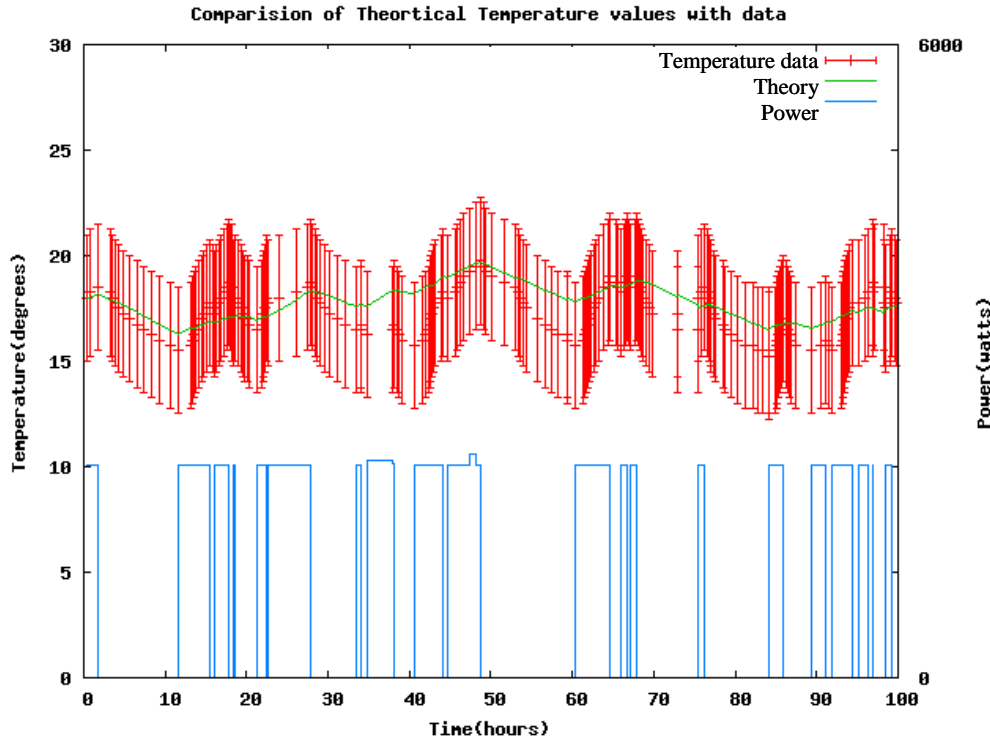


Figure 3.34-A – Shows a surface plot of the log of the likelihood for the two parameter distribution. Plots are shown at various different to make apparent the sampling focus about the maximum of the likelihood.



**Figure 3.34-B – Shows a surface plot of the log of the likelihood for the two parameter distribution. Plots are shown at various different to make apparent the sampling focus about the maximum of the likelihood.**



**Figure 3.35 – Plot showing the values of the data and the corresponding theoretically predicted values. In addition, the power function is also plotted for comparison.**

The value of  $\alpha = 0.013 \text{ hour}^{-1}$  is again similar order to that predicted made in section 3.1 of  $\alpha = 0.008 \text{ hour}^{-1}$ , while  $\beta = 1.9 \times 10^{-4} \text{ JK}^{-1}$  also compares reasonably favourably with the physical estimate of  $\beta = 3.2 \times 10^{-4} \text{ KJ}^{-1}$ . This value of  $\beta$  corresponds to an efficiency of 47% rather than the 80% used in our physical estimate a good indication that our initial estimate was too high. We also see that figure 3.35 shows a reasonable correspondence between the theoretically predicted temperature values and the data. However, while general trends predicted by the model are seen to track with those of the measured data reasonably well, we rarely get close correspondence at the more extreme points of the fluctuation. It is very likely that our model of the situation is too simplistic and that using more complex forms of the sources of heat and of the compartments response to heat we may get an improved correlation. Further investigations may come from increasing the complexity of our cooling model and adopting the multi-compartment approach mentioned in section 3.2. We may also wish to extend our model to include both sources of heating such as that from the sun or electrical devices within the room and perhaps a more appropriate spatially dependant form of the power delivered by heating.

### 3.4 Including the effect of sunlight on thermal variations

An example of a further source of heating which is likely to be important to temperature variation within a compartment is that of solar radiation. To develop a simple model of the power delivered by the sun we consider the incident power on a window of the room. For a window of area  $A$ , we assume that the power per unit area delivered by an incident flux of photons  $P_{Incident}(t)$ , can be related to the heating of the room by an efficiency coefficient  $\lambda$

$$\frac{dQ_{Solar}}{dt} = A\lambda P_{Incident}(t)$$

In the above expression the coefficient  $\lambda$  will be strongly related to the reflection coefficient of the glass and in general represents the proportion of normally incident radiation which is converted into useful heat. The expression for the incident power can be better understood by appreciating causes of variations in incident solar power over time.

To understand variations in incident power on a window it is crucial to appreciate the variation in the position of the sun in the sky over time. In general the position of the sun in the sky can be described by two angles, the solar altitude/elevation and the solar azimuth (see figure 3.41). Both of these angles will have an important effect on the intensity through different times of the day by virtue of the angular dependence they introduce into our expressions for normally incident power.

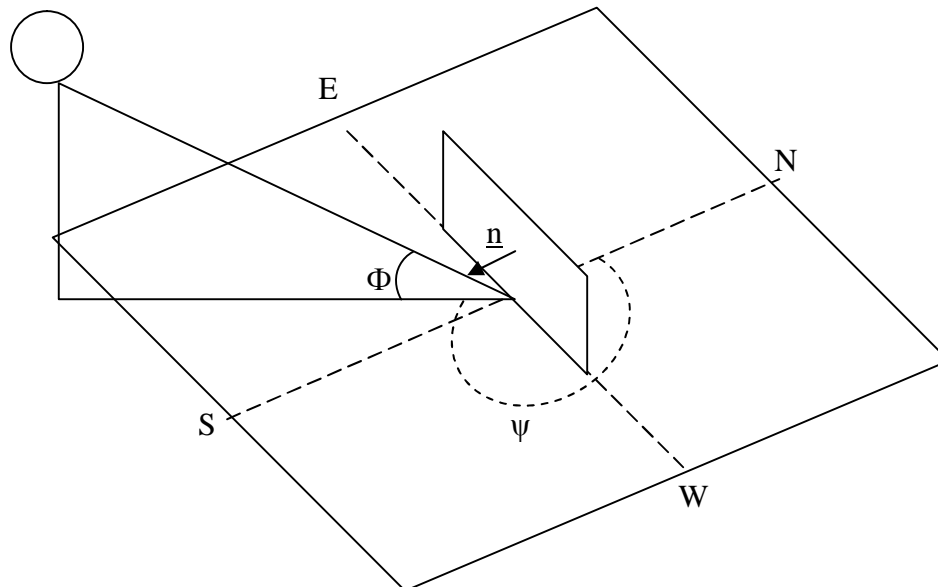


**Figure 3.41 – Shows the geometry of solar position in relation to a south facing window of with normal  $\underline{n}$ . Solar altitude  $\Phi$  and the azimuth  $\psi$  as functions of time can be seen in figure 3.42.**

The variation in the solar altitude will affect the intensity of incident power on a window perpendicular to the ground according the following expression:

$$P_{incident}(t) = P_{Average} \cdot \cos \Phi(t) \cdot \sin \psi(t) \cdot s(t)$$

Where the average solar intensity  $P_{Average}$  can be taken to be approximately  $1000 \text{ Wm}^{-2}$  and  $s(t)$  is the number of hours of sunshine per hour i.e. a measure of the sun shining or not. This will be a 'steppy' function looking similar to the previously described power generation. This expression is the resolved component incident power on surfaces perpendicular to the ground.

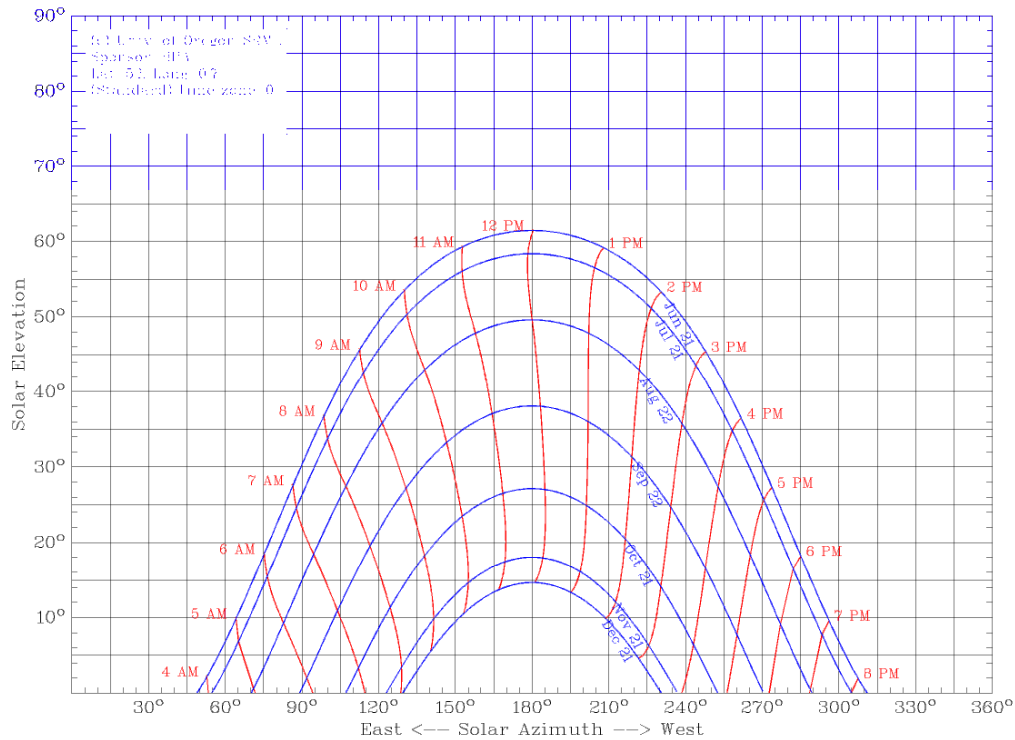


**Figure 3.42 - Sunchart showing the variation in solar altitude both at different times during the day and for different months during the year. This plot is a calculation specific to the geographical position of Cambridge [1C].**

The resultant modification to the differential equation must take into account the angular dependence of this sunshine term namely the differential equation will take the form

$$\frac{dT}{dt} = -\alpha(T(t) - T_0(t)) + \beta P(t) + \gamma \cos \Phi(t) \sin \psi(t) s(t)$$

Where  $\gamma$  has units  $\text{Ks}^{-1}$  and is given by:

$$\gamma = \frac{\lambda \cdot A \cdot P_{\text{Average}}}{C}$$

To provide an estimate of what we might expect  $\gamma$  to be we will first assume an average incident solar power of  $1000 \text{ Wm}^2$  [8]. We then take the area of the window to be approximately  $2 \text{ m}^2$  and  $\lambda$  to have a value of 0.5. Finally we use our calculated value of the rooms heat capacity,  $C_{\text{Total}}$  to obtain the estimate  $\gamma = 1.1 \times 10^{-4} \text{ Ks}^{-1}$

Again the simulation is first tested using toy data generated from known parameters. As we have moved to a 3 dimensional hypothesis space forming a plot of the likelihood is not feasible as it was before and so only a comparison the data with the theoretical prediction is provided (see Figure 3.43).

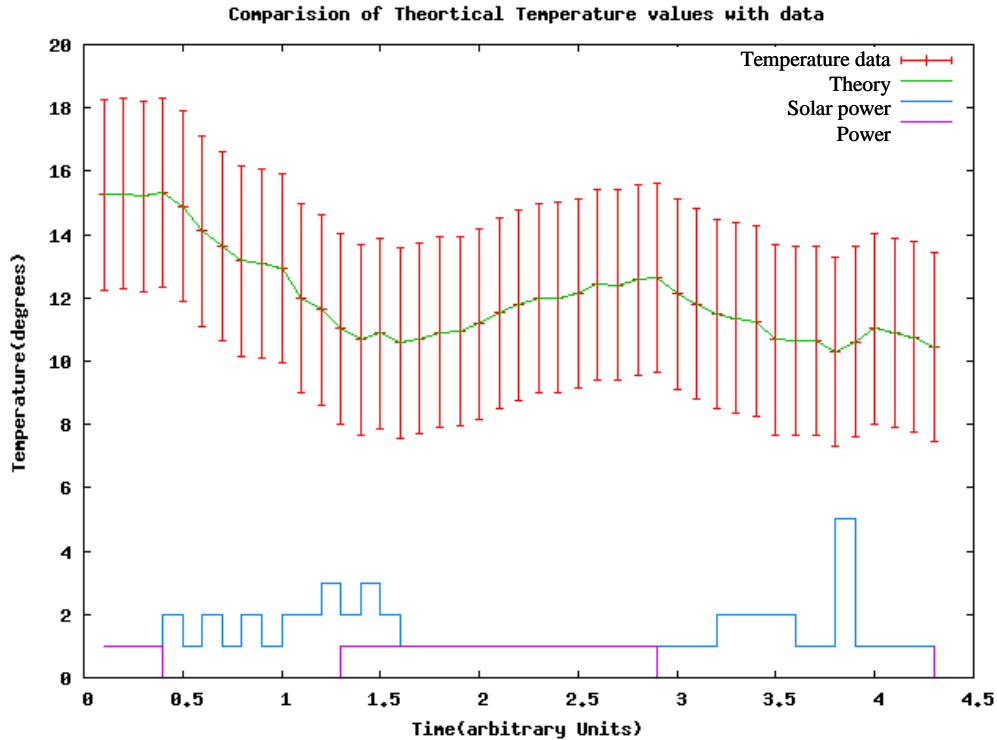


**Figure 3.43 – Plot of the comparison between predicted and actual temperature variation for generated toy data. Corresponding power and sunshine variation are also included for comparison (note these have arbitrary units).**

To investigate real building data we again appeal to the period in November where gas readings have been taken and so we have the data to incorporate both heating terms into the model. The inference simulation was again run and showed a maximum likelihood for Parameter values  $\alpha = 0.0105 \text{ hour}^{-1}$ ,  $\beta = 2.1 \times 10^{-4} \text{ KJ}^{-1}$  (or an efficiency of 52%) and  $\gamma = 2.78 \times 10^{-4} \text{ Ks}^{-1}$ . These values compare well with our previous physical estimates of  $\alpha = 0.008 \text{ hour}^{-1}$ ,  $\beta = 3.2 \times 10^{-4} \text{ KJ}^{-1}$  and  $\gamma = 1.1 \times 10^{-4} \text{ Ks}^{-1}$  for these parameters and suggest that some of the key trends that modelled are in fact relevant contributions to the temperature variation.

Figure 3.44, again provides a comparison between theoretical temperature values and the data. From this we again see that while our approach is predicting the general form of the variation it is not getting particularly close to the temperature more extreme parts of the variation. It should also be noted that the differences between this curve and that generated by just looking at the power of the gas fire on its own are reasonably small suggesting that for this compartment, over the period of time studied, solar radiation played a small role in the heating of the compartment. This was also found in the small differences in the value of the posterior for reasonably large variations in  $\gamma$ . For the reason we must again conclude that our model, while a useful guide to the relative importance of certain contributions would surely be much improved with a more detailed look at the sources of and responses to heat variation within the room. A possible improvement would be to run the experiment again at a time of year where the average solar intensity is higher.

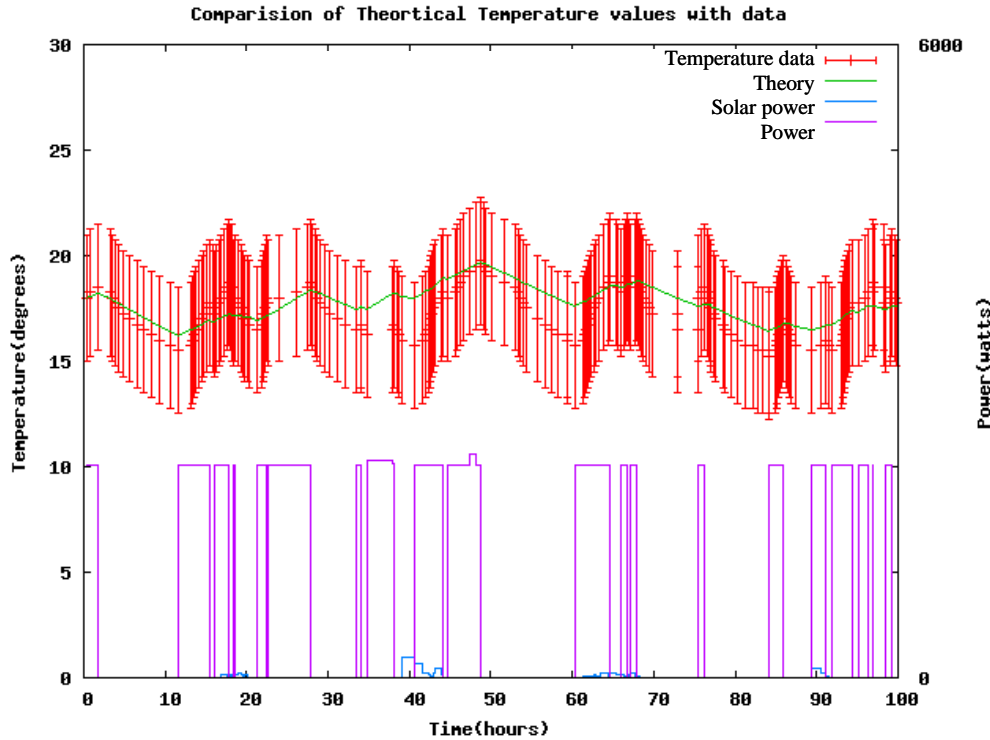


Figure 3.44 shows the comparison of temperature data against the theoretical values predicted for a model including the effects of sunshine as a source of heat.

#### 4. Conclusions

The aim of this project was to develop an empirical model of temperature variation within a building with the goal of using this to understand better the dynamics of energy usage. The models presented attempt to do this by considering simple representations of the most probable and obvious contributions to the heat budget

Heat losses were studied by considering the cooling of a room as being directly related to the temperature difference with the outside environment. This was then extended by including the additional effect of interaction with a structure with a much higher heat capacity than air, for example a wall. The models developed to understand cooling predicted the general trends well and showed reasonable agreement with appropriate physical estimates of there parameters. The observed small scale variations in the temperature are likely the result of a more complex mechanism of heat loss and were far less well predicted. It is suspected that a more general multi-compartment model allowing for interactions between each room within the building and the consideration of ventilation would better model heat losses and so account for more of the small scale variations in the temperature.

To consider the effect of sources of heat on the temperature variation of the compartment we first looked at the effect of the heating system, namely a gas fire considered to be delivering heat uniformly to the compartment. This was then extended to take into account the additional effect of solar radiation incident on a window of the room. The culmination of this model again predicted general trends in temperature variation to within 3 degrees. It is likely that including additional sources of heat and more importantly a more complex cooling model would lead to better prediction of temperature variation in buildings.

## 5. Appendices

### Appendix A – Numerical Integration

To obtain theoretical values of the temperature predicted by the various forms of differential equation governing temperature variation we use Euler’s method to integrate the differential equation numerically [9]. Euler’s method allows integration of the general form:

$$\frac{dT}{dt} = f(T, t)$$

Theoretical values of temperature are found by setting the initial conditions equal to the temperature and time at the first data point, and iterating until the time-step corresponding to the end of the dataset. The iterative formula is described as:

$$T_{i+1} = T_i + hf(T, t)$$

More complicated methods may offer better accuracy and stability, however for an appropriately size time step  $h$  this method is perfectly reasonable for datasets of the size we are using (typically not more than 200 values).

### Appendix B – Methods of data collection

Natural data has been collected from two primary sources throughout this project. The source of temperature data from rooms within buildings was provided using AlertMe wireless temperature sensors placed in the rooms, with the data being exported from the accompanying website [1A].

Data relating to external conditions outside of the building was collected from Cambridge weather station provided by Cambridge University Computer Science Laboratory weather station [1B]. Data relating to solar altitude and azimuth was provided by the solar radiation monitoring laboratory at the University of Oregon [1C].

### Appendix C – Calculating the Heat Capacity of a room

To find a value of the heat capacity of a room we will need to take a number of contributing factors into account. The first is from the air contained within the room. We can calculate the heat capacity of the air in the room using:

$$C_{air} = C_{volumetric} \times volume$$

Using a standard value of  $1.29 \text{ kJm}^{-3}\text{K}^{-1}$  for volumetric heat capacity and assuming the room volume to be  $30\text{m}^3$  we obtain  $C_{air} = 39000 \text{ JK}^{-1}$

The second contribution is that of the ‘stuff’ in a room (belongings and furniture etc...). To calculate the contribution of the ‘stuff’ in the room we approximate the specific heat capacity of all of objects to be of the similar of that of water, i.e.  $4200\text{Jkg}^{-1}\text{K}^{-1}$ . Estimating the total mass of all the stuff in the room as  $\sim 200 \text{ kg}$  we obtain:

$$C_{\text{Stuff}} = 840000 \text{ JK}^{-1}$$

A third Contribution may come from taking into account the heat capacity of the walls not interacting with the outside environment. Consider a Brick wall with specific heat capacity  $0.84 \text{ Jg}^{-1} \text{ K}^{-1}$ .

For a wall of volume  $5 \text{ m}^2$  and with the density of a material like brick at  $1.84 \times 10^6 \text{ gm}^{-3}$ , putting all these factors together with the specific heat capacity we get an additional contribution of  $9 \times 10^6 \text{ JK}^{-1}$

As a result of these contributions we obtain a total heat capacity of  $\sim 1 \times 10^7 \text{ JK}^{-1}$

## Appendix D – Source Code

Computer code is most useful in electronic form and as such is available on a CD submitted with this report.

## 1. References

1. MacKay, D.J.C. (2009) *Sustainable Energy – without the hot air*, pg 289. Cambridge: UIT Cambridge. Available free online <http://www.withouthotair.com>
2. MacKay, D.J.C (2003) *Information Theory, Inference, and Learning Algorithms*, pg 49. Cambridge: Cambridge University Press
3. MacKay, D.J.C (2003) *Information Theory, Inference, and Learning Algorithms*, pg 300. Cambridge: Cambridge University Press
4. Hanson, K.M. (2007) ‘Lessons about likelihood functions from nuclear physics’, *AIP Proceedings: Bayesian Inference and Maximum Entropy Methods in Science and Engineering*.
5. MacKay, D.J.C (2003) *Information Theory, Inference, and Learning Algorithms*, pg 312. Cambridge: Cambridge University Press
6. Neal, R.M. (2003) ‘Slice Sampling’, *The Annals of Science*, **31**, 3 705-767
7. MacKay, D.J.C. (2009) *Sustainable Energy – without the hot air*, pg 290. Cambridge: UIT Cambridge. Available free online <http://www.withouthotair.com>
8. MacKay, D.J.C. (2009) *Sustainable Energy – without the hot air*, pg 38. Cambridge: UIT Cambridge. Available free online <http://www.withouthotair.com>
9. Press, W.H. *et al.* (1992) *Numerical Recipes in C: the art of scientific computing, second ed.*, Cambridge: Cambridge University Press.

## Websites

[1A] - <http://www.alertme.com/>

[1B] - <http://www.cl.cam.ac.uk/research/dtg/weather/>

[1C] - <http://solardat.uoregon.edu/SunChartProgram>